

STATISTICAL POWER MEASUREMENT UNIT FOR AN 8MM-BAND TWO DIMENSIONAL SYNTHETIC APERTURE INTERFEROMETRIC RADIOMETER BHU-2D

Cheng Zheng^{*}, Xianxun Yao, Anyong Hu, and Jungang Miao

School of Electronics and Information Engineering, Beihang University, No. 37 Xueyuan Road, Haidian District, Beijing 100191, China

Abstract—An 8 mm-band two-dimensional Synthetic Aperture Interferometric Radiometer (SAIR) called BHU-2D has been developed by Electromagnetics Engineering Laboratory of Beihang University. The radiometer could obtain images in real-time benefiting from the adoption of a 1 bit/2level FPGA-based correlator array. The correlator array requires a group of Power Measurement Units (PMUs) to denormalize the correlation coefficients into visibility function samples. The design and implementation of the PMU in BHU-2D is presented in this paper. The PMU adopts a novel method based on probability statistics. The principle and quantitative error analysis of this power measurement method is presented. In order to verify the principle of the design, a sample board is manufactured and a series of validation experiments have been conducted. Measurement results have proved that the performance of the PMU could meet the requirements of SAIR systems. The PMU has been applied to BHU-2D and the result is satisfactory.

1. INTRODUCTION

Synthetic aperture interferometric radiometer was introduced in the late 1980s as an alternative to real aperture radiometer for earth observation. Through interferometry by an array of antennas, it realizes large equivalent aperture, and in turn achieves high resolution at low microwave frequencies with reduced mass and mechanical requirements [1]. A SAIR is in essential an array of interferometers. The interferometers measure the complex cross correlations between

Received 15 October 2012, Accepted 14 November 2012, Scheduled 21 November 2012

* Corresponding author: Cheng Zheng (zhengcheng@sina.com).

the signals received by each pair of antennas. Each complex correlation obtained by the SAIR can be called a sample of visibility function. In ideal condition, the visibility function could be expressed as the spatial Fourier transform of the brightness temperature within the field of view (FOV).

Electromagnetics Engineering Laboratory of Beihang University has been engaged with SAIR design and manufacture since 2004. A two-element interferometer operating at 8mm-band was developed in 2005, which proved the instrument concept was applicable. In 2006, a two-dimensional SAIR consisting of 10 receiving elements was developed. A T-shaped array and a disk array were applied to the 10 elements system to test the performance of the instrument [2, 3]. A series of brightness temperature images of the sun and a person were obtained by the system, which validated the configuration and image reconstruction algorithms. All signal processing subsystems of the instruments mentioned above consist of a group of receivers and data acquisition boards. Visibility function samples were generated by a computer after the experiments.

A new SAIR system called BHU-2D has been developed since 2006 [4]. BHU-2D consists of 24 receiving elements, which are located in a Y-shaped geometry. Accordingly, 276 complex cross correlations can be obtained. In order to achieve real-time brightness temperature imaging, an FPGA-based correlator array is included in BHU-2D.

For the purpose of reducing the complexity of the correlator array, 1 bit/2 level (1B/2L) correlator is selected. However, 1B/2L correlator only gives the correlation coefficient of the input signals [5]. Consequently, the power of the input signals are required to denormalize the correlation coefficients into visibility function samples. PMU is the component to measure the power of the input signals of the correlator. PMU can be implemented in several ways: in MIRAS and HUT-2D a group of detectors are included to obtain the power information, while in GeoSTAR 8 bit analogue to digital converters (ADCs) are adopted to monitor the power of the signals [6–8]. This paper introduces a power measuring method applied to the PMU of BHU-2D, which is based on probability statistics. The PMU adopts a digital method, from which the PMU could achieve better linearity than a detector does. Furthermore, the PMU requires only one threshold, which is simpler than an ADC based power meter. The experimental results of the PMU, presented in this paper, have proven that the method could meet the requirements of SAIR systems.

2. POWER MEASUREMENT METHOD

The requirements of the PMU in SAIR systems are different from the one in some other systems. The PMUs in SAIR systems usually work with low dynamic range and high linearity. The accuracy of the PMU should be managed within 1% (about 0.04 dB) [6]. In order to reserve some margin, 0.5% is applied to the discussion below.

2.1. Statistical Model

A radiometer is a passive instrument that measures the spontaneous electromagnetic radiation of the object. Consequently, the input signals of the correlator for a given target could be formulated as a stationary, ergodic, zero mean Gaussian random process $V(t)$. The probability density function of $V(t)$ can be expressed as

$$f(v) = \frac{1}{\sqrt{2\pi}\sigma} \exp\left\{-\frac{v^2}{2\sigma^2}\right\} \quad (1)$$

where v is a sample of $V(t)$ and σ^2 is the variance of the signal. The power of the signal can be expressed as

$$P = \frac{\sigma^2}{Z} = k(T_A + T_R)BG \quad (2)$$

where $Z(\Omega)$ is the impedance of matching load, $k = 1.38 \times 10^{-23} (J/K)$ is Boltzmann constant, B (MHz) and G are the bandwidth and the gain of the radiometer respectively, $T_A(K)$ and $T_R(K)$ are the antenna temperature and equivalent noise temperature of the radiometer respectively. Equations (1) and (2) show that $f(v)$ is related to P and the power of the signal could be measured statistically. If we set a threshold and measure the right tail probability of the signal, the power of the signal could be calculated.

Assume a threshold V_T is an element of the sample space Ω of $V(t)$. The probability of the event that $\{V > V_T\}$, which is called right tail probability, could be calculated by the equation

$$P\{V > V_T\} = \int_{V_T}^{+\infty} f(v) dv \quad (3)$$

Then the probability that $V(t)$ is between $(V_T, +\infty)$ could be expressed as

$$P_\mu = \left[1 - \operatorname{erf}\left(\frac{\mu}{\sqrt{2}}\right)\right]/2 \quad (4)$$

where $\operatorname{erf}(x) = \int_0^x \exp\{-t^2\} dt$ is the error function, and $\mu = V_T/\sigma$ is normalized threshold. The variance of $V(t)$ could be estimated by

inversion of Equation (4)

$$\sigma_e^2 = \left(\frac{V_T}{\mu} \right)^2 = \left(\frac{V_T}{\sqrt{2} \operatorname{erf}^{-1}(1 - 2P_\mu)} \right)^2 \quad (5)$$

Consequently, it is possible to estimate the power of the signal when the probability of $\{V > V_T\}$ is given.

Practically, input signals will be converted into digital signals in the signal processing subsystems of the SAIRs in order to reduce the complexity and power consumption of the correlator array. In this situation, right tail probability P_μ could be estimated by

$$\hat{P}_\mu = \frac{M_1}{M} \quad (6)$$

where M is the total sample number of digital signal and M_1 is the number of samples that meets the condition $\{V > V_T\}$. Therefore, for a given M and V_T , the power of the signal could be estimated by measuring M_1 .

2.2. Error Analysis

When measured by Equation (6), \hat{P}_μ follows Gaussian distribution [9]

$$\hat{P}_\mu \sim N \left(P_\mu, \frac{P_\mu(1 - P_\mu)}{M} \right) \quad (7)$$

as long as the samples are uncorrelated. According to the error propagation formula, the standard deviation of the power σ_e^2 could be expressed as

$$\gamma = 2\sqrt{\pi} \frac{e^{[\operatorname{erf}^{-1}(1-2P_\mu)]^2}}{\operatorname{erf}^{-1}(1-2P_\mu)} \sqrt{\frac{P_\mu(1-P_\mu)}{M}} \cdot \sigma^2 \quad (8)$$

Equation (8) shows that the relative error of the power measuring method depends on the total sample number M and right tail probability P_μ . In practice, M equals to the product of sampling rate and integration time. In BHU-2D, the sampling rate is 200 MHz and the integration time can be adjusted between 0.1s and 20s, which correspond to $M = 2^{24} \sim 2^{32}$. The relative power estimate error with respect to right tail probability for $M = 2^{24} \sim 2^{32}$ is illustrated in Fig. 1. As could be seen in the figure, the relative power estimate error

$$\varepsilon = \frac{\gamma}{\sigma_e^2} \quad (9)$$

could be managed within 0.5% for a wide range of probability P_μ .

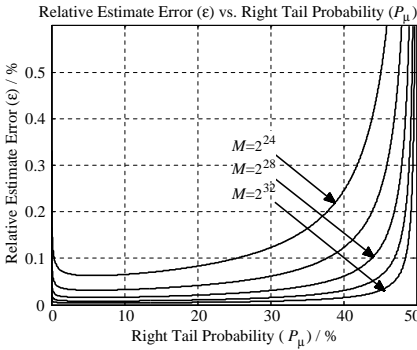


Figure 1. Power estimate error with respect to right tail probability for different total sample number.

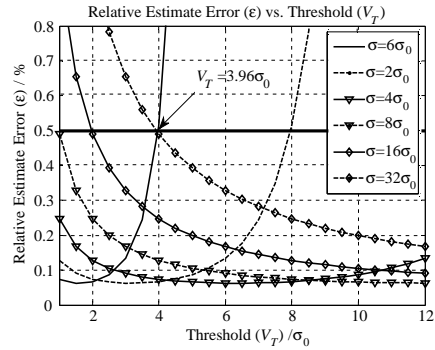


Figure 2. Power estimate error with respect to threshold for different input signal power ($M = 2^{24}$).

2.3. Dynamic Range and Operating Point

According to Equation (8), the dynamic range of the method could be determined for a given ε and M . Correspondingly, an operating point of V_T could be selected. In order to draw the dynamic range of the PMU, σ_0^2 is assumed as the minimum input power of the PMU and then the maximum input power could be expressed, from which the dynamic range could be calculated. Figure 2 illustrates the relative estimate error ε with respect to the threshold V_T for a group of different input power σ^2 . Both of σ and V_T are normalized by σ_0 . In the figure, $M = 2^{24}$ is given as an example because it is the worst case for $M = 2^{24} \sim 2^{32}$. The figure shows that $\varepsilon < 0.5\%$ could be achieved when σ is between σ_0 and $32\sigma_0$ in the condition of $V_T = 3.96\sigma_0$. Then the operating point of PMU could be set as $V_T = 3.96\sigma_0$ and the dynamic range is about $20 \log 32 = 30$ dB. In BHU-2D, the dynamic range required is about 4.4 dB for $T_R \approx 300$ K and $T_A = 30 \sim 600$ K considering the condition of noise injection calibration. The dynamic range of PMU is sufficient for BHU-2D.

2.4. Calibration

The block diagram of the PMU is illustrated in Figure 3. The comparator and counter can obtain the frequency of $\{V > V_T\}$, then look up table can give the power based on M_1 . For a given V_T and M , the look up table is generated by combining Equations (5) and (6). The quantization of the input for the look up table is determined by

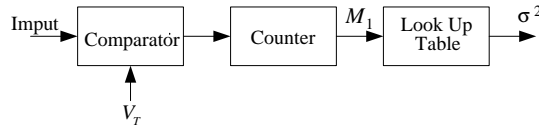


Figure 3. Block diagram of the PMU.

the relative error required.

Figure 3 shows that the output error of PMU depends on the offset of V_T when the look up table is accurate enough. Consequently, V_T is the only parameter that requires calibration, which means one point calibration could be used. Fortunately, radiometers need at least two points to obtain the gain and receiver noise temperature. We only need to concentrate on the calibration of PMU and assume that other errors could be neglected. If there is a calibration input signal whose variance is σ_c^2 . The calibrated threshold could be expressed as

$$\hat{V}_T = \sqrt{2} \operatorname{erf}^{-1}(1 - 2P_c) \sigma_c \quad (10)$$

where P_c is the right tail probability when calibration signal is measured, \hat{V}_T the estimate of the threshold. Considering σ_c provided by an external calibration load. and P_c can be measured by longer integration time and their errors are negligible. Consequently, the signal power to be measured could be calculated by Equations (5) and (10)

$$\sigma_x^2 = \left(\frac{\operatorname{erf}^{-1}(1 - 2P_c) \sigma_c}{\operatorname{erf}^{-1}(1 - 2\hat{P}_x)} \right)^2 \quad (11)$$

where \hat{P}_x is the estimate of right tail probability when the signal under test is measured. Because σ_c and P_c is accurate enough, the error of σ_x^2 is come from Equation (8) unless the quantization of the look up table is not small enough.

3. DESCRIPTION OF THE PMU IN BHU-2D

The PMU of BHU-2D is embedded in the data acquisition unit, which is shown in Figure 4. The data acquisition unit consists of 16 ADCs and a FPGA. The input signals are quantized by the ADCs and the data can be stored for further analysis. The sampling frequency and resolution of the ADCs are 200 MHz and 8 bits respectively. The comparator and counter of the PMU are implemented in the FPGA. The comparator in the FPGA is a digital one and the threshold is



Figure 4. The data acquisition unit in BHU-2D.

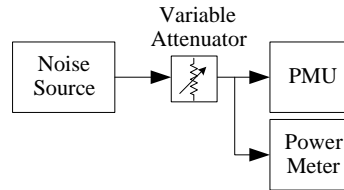


Figure 5. The setting of the validation experiment of PMU.

selected from the ADC output codes. Consequently, the upper limit voltage level of the threshold code could be considered as a real analogue threshold and the digital comparator could be equivalent to an analogue one. In the future, the data acquisition unit will be improved and the ADCs will be replaced by comparators in order to reduce the complexity and power consumption.

The parameters in the PMU are set as $M = 10^8$ and $V_T = 42 \text{ LSB}$, where LSB is the least significant bit of the ADC. The total sample number corresponds to a typical integration time of 0.5 s. The threshold can be concluded from Figure 2. As can be seen, the relative errors of the input signal $\sigma = 2\sigma_0$ and $\sigma = 4\sigma_0$ are lower than the others in the condition of $V_T = 3.96\sigma_0$. Then the operating range can be set between $\sigma_{\min} = 2\sigma_0$ and $\sigma_{\max} = 4\sigma_0$, which is large enough for BHU-2D. Consequently, V_T can be approximated by σ_{\max} . For the purpose of protecting the 8-bit ADC, the peak-peak value of the input signal should be lower than 255 LSB, which corresponds to $V_T = \sigma_{\max} = 255/6 = 42 \text{ LSB}$ since the signal follows Gaussian distribution.

4. EXPERIMENTS

Validation experiments for the PMU have been carried out and some results will be shown in this section. The settings of the experiment are illustrated in Figure 5. The noise source generates a band limited signal, whose bandwidth is 160 MHz. The variable attenuator is used to adjust the power of the signal. A power meter is included to measure the actual power of the input signal in order to make a comparison. During the experiment, a group of signals with different power are measured and the results are listed in Table 1.

For a given input signal, PMU measures the power of the signal for 100 times. The average and standard deviation of the results are recorded in Table 1. The indications are normalized in LSB because the offset error and full scale error of the ADC is not calibrated. As is shown in Table 1, the relative error of the outcome is less than 0.1%.

In order to calibrate the PMU, the measurements of the power meter are recorded as true value in Table 1 and a linear regression is applied to the first two columns. The result of the regression is shown in Figure 6 and the approximate equation is

$$P_{in} = 0.3698P_{ind} + 5.0610 \tag{12}$$

Table 1. Test results for the PMU of BHU-2D.

True value (μW)	Average of 100 measurements (LSB^2)	Standard deviation of 100 measurements (LSB^2)	Relative error (%)
130.5	343.0	0.2	0.06
163.9	431.5	0.3	0.06
201.3	529.8	0.3	0.05
241.9	639.2	0.4	0.06
289.9	767.6	0.5	0.06
331.7	880.6	0.6	0.06
377.3	1003.7	0.5	0.05
439.0	1173.8	0.7	0.06
511.9	1375.2	1.0	0.07

Relationship Between The True Value And Indicated Value of The PMU

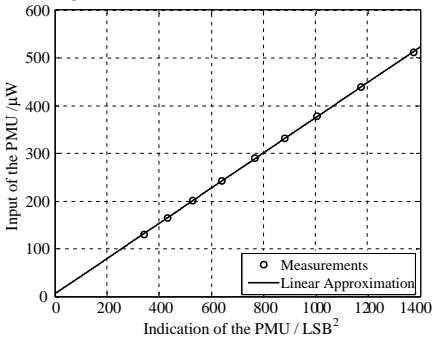


Figure 6. Relationship between the true value and indicated value of the PMU.

Relationship between the relative error and input of the PMU

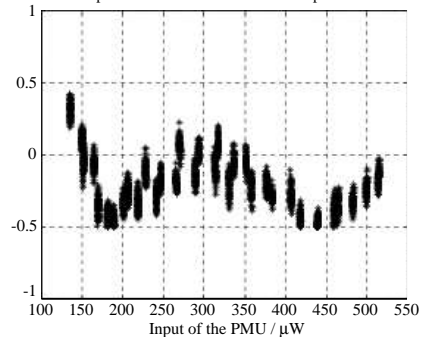


Figure 7. Relationship between the relative error and input of the PMU.

where P_{in} is the true value and P_{ind} the indication of the PMU. In Equation (12), the offset of the indication may be caused by the imperfection of the hardware and instrument. The slope indicates that one LSB of the ADC is approximately 4.3 mV, which corresponds to $V_T = 42 \text{ LSB} = 180.6 \text{ mV}$. Actually, the offset and V_T is less important because the linear calibration equation including the gain and noise temperature of the receiver could be obtained by two points calibration as long as the linearity of the PMU is guaranteed. Consequently, the correlation coefficient between the true value and average of measurements is calculated. The result is 0.9999, which features the linearity of the PMU.

In order to verify the calibrated performance of the PMU, another group of input signals is measured. The indications of the PMU are substituted in Equation (12) and the linear approximations are obtained. The relative errors between the linear approximations and the true values are shown in Figure 7. As can be seen, the relative error measured by the PMU is less than 1%.

5. CONCLUSIONS

A statistical power measuring method for SAIR is presented in this paper. The method requires only one comparator and one counter. This structure is particularly suitable for low level quantization systems. For example, in a 3 level correlator system, each channel requires two comparators to digitize the signal. One of the comparators can be shared with the PMU. Meanwhile, a group of counters are more suitable for Very Large Scale Integration (VLSI) implementation than a group of detectors and ADCs. Besides, the dynamic range of the method can be up to 30 dB, which is large enough for a microwave radiometer.

The new method is applied to the design of the PMU in BHU-2D. Results show the relative error of the PMU is less than 1%, which meets the requirements of SAIR systems. In the future, our efforts will focus on low level quantization systems including 1B/2L correlator array and one threshold PMU without high resolution ADCs.

REFERENCES

1. Le Vine, D. M., A. J. Griffis, C. T. Swift, and T. J. Jackson, "ESTAR: A synthetic aperture microwave radiometer for remote sensing applications," *Proc. IEEE*, Vol. 82, No. 12, 1787–1801, Dec. 1994.

2. Xue, Y., J. Miao, G. Wan, A. Hu, F. Zhao, and H. Wu, "Prototype development of an 8 mm band 2-dimensional aperture synthesis radiometer," *Proc. IGARSS*, Vol. 5, V-413–V-416, Boston, MA, Jul. 7–11, 2008.
3. Xue, Y., J. Miao, G. Wan, A. Hu, and F. Zhao, "Development of the disk antenna array aperture synthesis millimeter wave radiometer," *Proc. ICMMT*, Vol. 2, 806–809, Nanjing, China, Apr. 21–24, 2008.
4. Miao, J., "Microwave aperture synthetic radiometer and the passive millimeter wave imager of Beihang University," *Proc. ICMTCE*, 7, Beijing, China, May 22–25, 2001.
5. Ruf, C. S., "Digital correlators for synthetic aperture interferometric radiometry," *IEEE Trans. Geosci. Remote Sens.*, Vol. 33, No. 5, 1222–1229, Sep. 1995.
6. Martin-Neira, M., I. Cabeza, C. Perez, M. A. Palacios, M. A. Guijarro, S. Ribo, I. Corbella, S. Blanch, F. Torres, N. Duffo, V. Gonzalez, S. Beraza, A. Camps, M. Vall-llossera, S. Tauriainen, J. Pihlflyckt, J. P. Gonzalez, and F. Martin-Portueras, "AMIRAS — An airborne MIRAS demonstrator," *IEEE Trans. Geosci. Remote Sens.*, Vol. 46, No. 3, 705–716, Mar. 2008.
7. Rautiainen, K., H. Valmu, P. Jukkala, G. Moren, and M. Hallikainen, "Four-element prototype of the HUT interferometric radiometer," *Proc. IGARSS*, Vol. 1, 234–236, Hamburg, 1999.
8. Tanner, A. B., W. J. Wilson, P. P. Kangaslahti, B. H. Lambrigsten, S. J. Dinardo, J. R. Piepmeier, C. S. Ruf, S. Rogacki, S. M. Gross, and S. Musko, "Prototype development of a geostationary synthetic thinned aperture radiometer, GeoSTAR," *Proc. IGARSS*, Vol. 2, 1256–1259, Anchorage, AK, Sep. 20–24, 2004.
9. Kay, S. M., *Fundamentals of Statistical Signal Processing, Volume II: Detection Theory*, Upper Saddle River, 45–46, Prentice Hall, NJ, 1993.